IT-CsF1 TAI EVALUATION
MJD 54774-54789 (November the 4th - 19th 2008)

Introduction

During the period MJD 54774.0-54789.0, INRiM has evaluated the frequency of its Hydrogen Maser IT-HM2 (BIPM code 1401102) using the Cs fountain primary frequency standard IT-CsF1. The evaluation procedure of the fountain standard follows the general procedures reported in [1, 2]; we report here details on the Type A and Type B uncertainty evaluation, together with the internal transfer uncertainty (including the contribution of dead time).

IT-CsF1 Accuracy Evaluation

Black Body Radiation Shift $\Delta\nu_{BBR}$

The evaluation of the Blackbody Radiation (BBR) Shift $\Delta\nu_{BBR}$ requires to know the effective BBR temperature T experienced by the atoms along their ballistic flight. For the calculation of T, we interpolate the temperature data coming from four thermocouples positioned along the drift tube with a polygonal curve and then we calculate the average radiation temperature experimented by the atoms at a given position (integrated over the solid angle); in this way it is possible to take into account also the effect of the two "holes" in the blackbody radiator, the upper window and the hole in the microwave cavity. The values obtained at different elevations inside the fountain drift tube are then used to calculate the time averaged radiation temperature seen by the atoms along their ballistic flight. See the discussion reported in [3] for details.
To evaluate $\Delta\nu_{BBR}$ from the effective temperature T we follow the well known relation discussed for example in [3] and reported here below; the leading coefficient β here used is calculated using results presented in [4]; the coefficient ε is taken from [5].

$$\Delta\nu_{BBR} = \beta\,(T/300)^4 \cdot [1+\varepsilon(T/300)^2]$$

$$\beta = (-1.711 \pm 0.003) \cdot 10^{-14}$$

$$\varepsilon = 0.014$$

$$T = 66.1 \pm 1.0\ ^\circ C = 339.3 \pm 1.0\ K$$

$$\Delta\nu_{BBR} = (-28.5 \pm 0.3) \cdot 10^{-15}$$

Gravitational Red Shift $\Delta\nu_{RS}$

Gravitational redshift at the IT-CsF1 location was accurately calculated during 2006 and the result from that activity is used here to correct the TAI calibration data. These evaluation data take advantage of some refined gravimetric data, coming from an accurate Geoid regional model and levelling techniques together with precise geometrical measurements of the vertical position of IT-

CsF1 with respect to the geodetic reference markers. A detailed description of this work is reported in a Metrologia paper [6].

$$\Delta\nu_{RS} = \gamma \cdot h$$

$$\gamma = 1.09 \cdot 10^{-16}\ m^{-1}$$

$$h = 239.43 \pm 0.03\ m$$

$$\Delta\nu_{RS} = (+26.10 \pm 0.01) \cdot 10^{-15}$$

Quadratic Zeeman Shift $\Delta\nu_Z$

The effective C-field experienced by the atoms (B_0) along their trajectory is calculated (see [1] for details) from a field map which is obtained measuring the low frequency magnetic resonance transitions when the atoms are at the apogee; the map is completed launching the atoms at different apogee heights.

The C-field map obtained after the evaluation period (on Oct 2008) is reported in the figure 1 and it was used to calculate the quadratic Zeeman shift by mean of a field integration over the flight time. Reference for the value of the quadratic Zeeman constant K is [7].

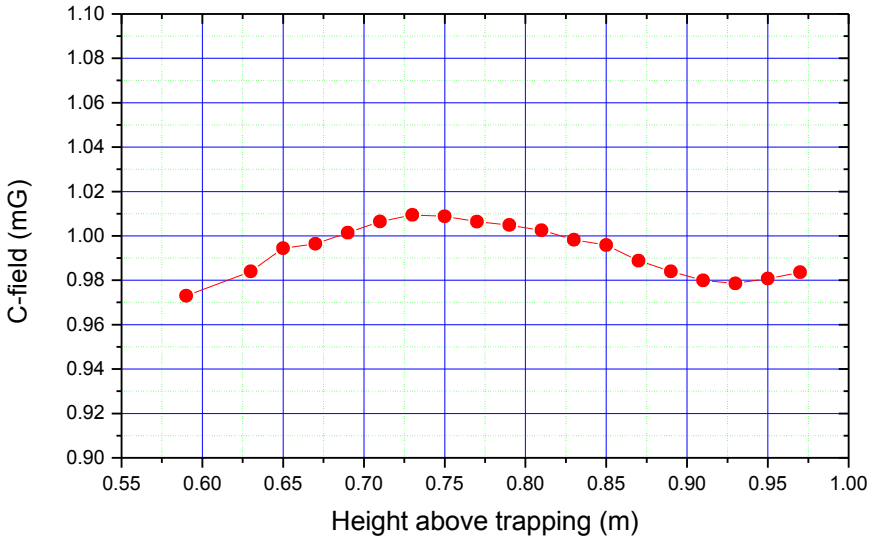

Figure 1. C-field map.

The uncertainty associated to the magnetic field was derived with three independent methods.

First, we evaluated the frequency instability of the clock locked on the central fringe of the magnetic sensitive transition F=3, m_F=-1→ F=4, m_F=-1. This yields to a value that is better than $5 \cdot 10^{-12}$ over one day of measurement. Consequently the instability on the clock transition is $< 1 \cdot 10^{-17}$

Second, the long term instability of the C-field was evaluated comparing two mapping results (March and May 2008). These two results differ by $1.4 \cdot 10^{-16}$. Adopting a conservative approach, this value is considered an estimation of the stability of dc quadratic Zeeman shift during this run.

Third, the uncertainty associated with the map prediction was evaluated. The C-field map is used to locate the central fringe of the F=3, m_F=-1→ F=4, m_F=-1 line. The numerical result agrees with that obtained following its position at increasing heights better than 0.3 Hz, yielding to a value for the uncertainty on the clock transition frequency of $4 \cdot 10^{-17}$.

The heater used to frequency tune the Ramsey cavity and to stabilize the drift tube temperature is powered with an audio-frequency generator (70 kHz) to avoid the penetration of the generated magnetic field inside the drift tube.

The heater is operated cw during the whole operation cycle of the fountain, in order to prevent a dynamic end-to-end phase shift [6] caused by a temperature modulation of the cavity synchronous with the Ramsey cycle.

Although shielded by several skin depths, a residual rms magnetic field produced by the audio frequency generator could penetrate inside the drift tube, causing a quadratic Zeeman shift of the clock transition frequency.

A calibration of this effect is performed feeding the part of the heater around the drift tube with a calibrated dc current, while the cavities are kept on resonance by the part of the heater around the cavities only (cw at 70 kHz as usual), where the thickness of the copper is larger and the shielding effect is estimated higher by several orders of magnitude.

We measured the magnetic field generated by the heater coils observing the frequency shift of the F=3,m_F=-1→ F=4,m_F=-1 transition, then we use this value to evaluate the residual magnetic field in the ac condition. The calibration shows that the ac Zeeman shift is less than $4 \cdot 10^{-17}$.

The total uncertainty on the Zeeman shift correction (dc and ac together) is then conservatively stated as $1 \cdot 10^{-16}$. Since we are using the previous mapping, the uncentainty has been enlarged to $3 \cdot 10^{-16}$ to take ainto account possible drifts of the C-field in agreement with the long term field stability as measured in the last 5-years.

$$\Delta\nu_Z = K \cdot B_0^2$$

$K = 427.45\ \mathrm{Hz/T^2}$

B_0, C-field as calculated with the map

$$\Delta\nu_Z = (+45.6 \pm 0.3) \cdot 10^{-15}$$

Collisional Shift

The collisional shift is evaluated using a continuous differential measurement during the whole period. The fountain is operated alternatively at high (HD) and low (LD) atomic density and the HM frequency measured in the two configurations is compared . As it was reported in [1], the ratio between the atomic density and the total number of detected atoms is assumed to be constant, then we can state that the collisional frequency shift is proportional to the number of detected atoms.

The differential measurement provides a collisional coefficient which is used to correct the spin-exchange shift on a few-hours basis with the proper density value as obtained by the detected signal.

During the present evaluation, the fountain is operated at LD or HD density using the MOT loading time (70 ms and 300 ms respectively at LD and HD) as a control parameter: the resulting ratio between the number of detected atoms in the two configurations was about 4. The fountain was continuously operated alternating 20640 s in the LD and about 6450 s in the HD configuration.

The HM frequency was then extrapolated to the zero atomic density condition, via the relation [2]:

$$y_0 = \frac{R}{R-1} y_{LD} - \frac{1}{R-1} y_{HD} \quad (1)$$

where y_0 is the zero density extrapolation, y_{LD} and y_{HD} are the frequency in LD and HD condition, R is the ratio between the number of atoms in HD configuration (N_{HD}) and the number of atoms in LD configuration (N_{LD}).
The y_0 extrapolation is calculated for each couple of LD-HD runs (total duration 27000 s), allowing a high level rejection of the effects (long term fluctuations of HM frequency, MOT loading efficiency and atom detection efficiency) which can introduce biases to the y_0 value calculated with (1).
The type A uncertainty associated to the measurement is then obtained from equation (1):

$$\sigma^2_{y0} = \left(\frac{R}{R-1}\right)^2 \sigma^2_{yLD} + \left(\frac{1}{R-1}\right)^2 \sigma^2_{yHD} + \sigma^2_R \left(\frac{y_{LD} - y_{HD}}{(R-1)^2}\right)^2 \quad (2)$$

Another contribution to the collisional shift uncertainty is reported in the Type B budget. This contribution is mainly due to the hypothesis about the linear relation between the atomic density and the detected signal and to a non-complete rejection of long term effects. This assumption is evaluated to be correct at the level of 20% .

During the present evaluation, the average value of the cold collision relative frequency shift and the associated type B uncertainty were:

$$\Delta\nu_{Coll} = (-1.3 \pm 0.2) \cdot 10^{-15}$$

Other Shifts

The actual influence of other shifts resulting from several physical and technical effects was carefully investigated during the most recent history of IT-CsF1. The contribution of these shifts is either negligible or not easily modelled and then no correction is applied for. Only an uncertainty contribution is provided for these effects, reflecting the estimation of their maximum values during the fountain operation.
These shifts, either theoretically estimated or measured, are [1,2]

- Resonant light shift
- Distributed cavity shift
- Dynamic end-to-end phase shift [8]
- Cavity pulling
- Relativistic Doppler shift
- Synthesizer and numerical loop errors
- Microwave leakage and power-related shifts

In order to estimate the shift and the uncertainty contributions of the microwave leakage during the operation of IT-CsF1, all the possible sources of microwave leakage were carefully surveyed. Leverage tests, conducted operating the fountain with a high microwave power level, provide an estimation of the possible leakage shift.
As it was recently reported [9], the relation between the microwave field amplitude and the leakage induced shift is not linear and can be dramatically different if the leakage occurs between the two Ramsey interrogations or after the second one, before the detection stage.

For these reasons, leverage tests were designed following the theory reported in [9], and different tests were conducted to estimate the shift due to the leakage during different stages of the fountain cycle.
In particular, driving the fountain at high microwave power, there is an evidence of a microwave leakage occurring during the time interval between the second Ramsey pulse and the detection. Fountain measurements with $\pi/2$, $3\pi/2$, $5\pi/2$ pulses provide results in agreement with the theory reported in [9]. Further differential measurements, involving the fountain operating at microwave power higher than normal ($3\pi/2$ and $5\pi/2$ pulse), took place for some days immediately before the main fountain run, which was operated with density shift differential measurements. Total accumulated time for this leakage test was about 3 days. Results coming from the $3\pi/2$-$5\pi/2$ differential measurements were then used to estimate the leakage shift using the theory reported in [9] (leakage shift at $\pi/2$ is about 1/8 with respect to the differential leakage shift between $5\pi/2$ and $3\pi/2$). The estimation of the microwave leakage shift is $< 0.5 \cdot 10^{-15}$

Summary of accuracy evaluation

Effect	**Shift (10^{-15})**	**Uncertainty (10^{-15})**
2nd order Zeeman Shift	+45.6	0.3
Blackbody Radiation Shift	-28.3	0.3
Gravitational Red Shift	+26.1	0.01
Microwave Leakage Shift	--	0.5
Collisional Shift (Systematic)	-1.3 (*)	0.2
Other shifts	--	0.1
Total	**+43.4**	**0.7**

Table 1. Summary of corrected and uncorrected shifts and uncertainty budget for IT-CsF1, MJD 54774-54789. (*) Average value, not accounted for the total correction reported in the last line.

Evaluation of the average frequency y(IT-CsF1)-y(HM2)

During the reported evaluation period, the H-maser HM2 (BIPM code 1401102) was used as local oscillator; the other one (BIPM code 1401101) was not available during the evaluation period.

The average frequency *y(IT-CsF1)-y(HM2)* over the period MJD 54774-54789 was calculated with a linear fit on the *y(IT-CsF1)-y(HM2)* data, coming from each individual fountain runs corrected only for the collisional shift. As these data have different Type A uncertainties, we used a weighted least square algorithm. The fit method was chosen because fountain dead (lost) time is unavoidable during the evaluation period, and the dead time intervals are neither evenly spaced nor symmetric with respect to the centre of the evaluation period. In these conditions, dead time would have biased an estimation derived by a standard average. Epoch distribution of fountain dead time is reported in Figure 2.

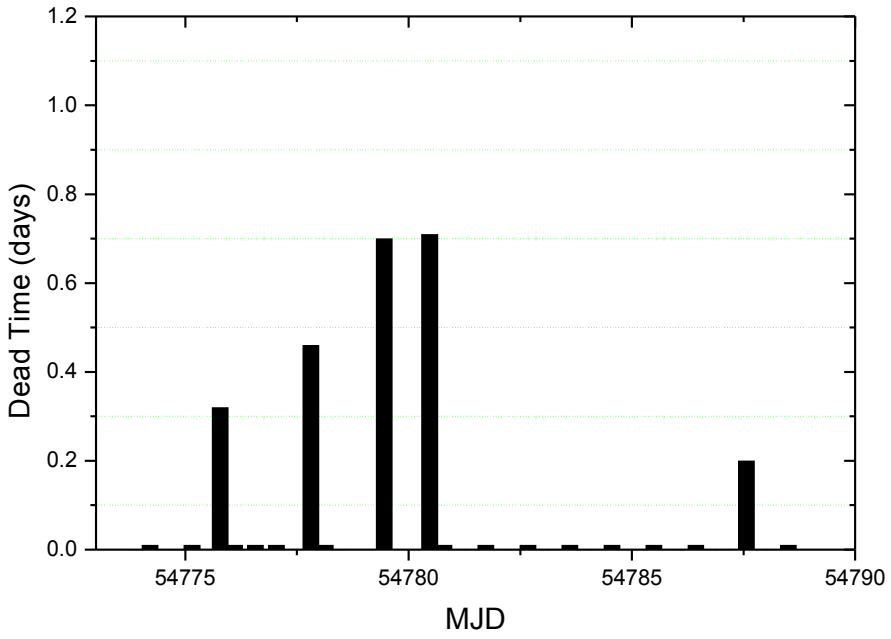

Figure 2. Epoch distribution of the dead time during the present evaluation.

y(IT-CsF1)-y(HM2) data are fitted with the linear model:

$$Y = At + B \tag{1}$$

The choice of a linear model takes into account the fact that the HM2 frequency has shown a very stable drift in the past two years within periods even larger than 40 days. Moreover, we tried to fit the data with a quadratic model; in this case the second order coefficient estimated by the fit was compatible with zero.

The estimation of the average frequency *y(IT-CsF1)-y(HM2)* during the evaluation interval is $Y|_{t=t0}$ where t_0 is the evaluation period centre (MJD 54781.5 in this particular case). If the epoch coordinate origin is taken on the centre of the evaluation interval, the coefficient B, as it is estimated by the weighted least square algorithm, corresponds to the estimation of the average frequency *y(IT-CsF1)-y(HM2)* during the evaluation interval.

The linear fit is weighted on the squared Type A uncertainty of each *y(IT-CsF1)-y(HM2)* datum. The uncertainty of each datum includes both the uncertainty due to the fountain stability and the uncertainty due to the collision shift evaluation (Type A contribution). The uncertainty associated to the average frequency estimation *y(IT-CsF1)-y(HM2)* and reported as Type A, is the uncertainty of the coefficient B as it is estimated by the weighted least square algorithm. Figure 3 reports *y(IT-CsF1)-y(HM2)* data, corrected only for the density shift and not the total shift reported in the last line of Table 1, and the linear fit curve.

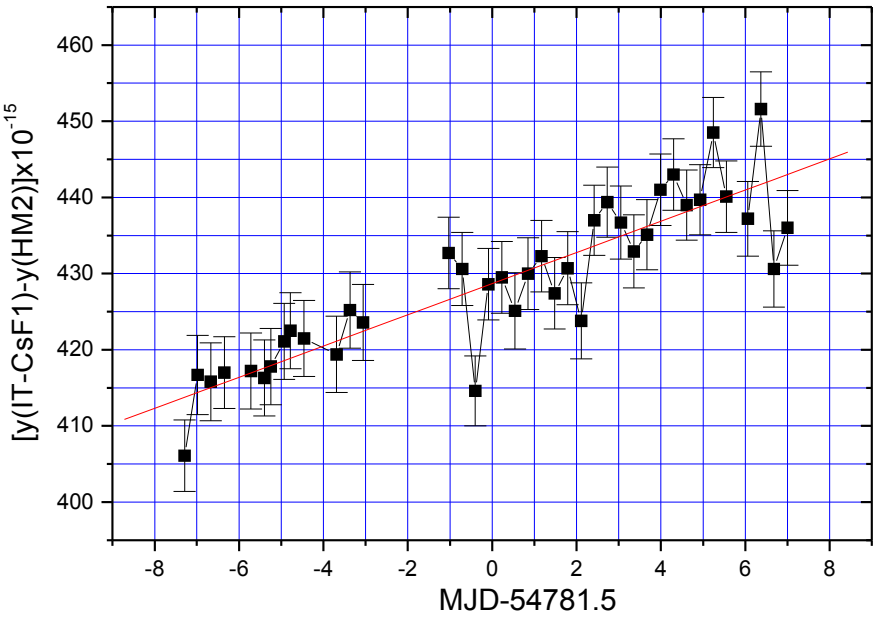

Figure 3. *y(IT-CsF1)-y(HM2)* data (squares) and the linear fit curve (straight line).

The linear regression provides the best estimation when the expression (1) is the correct model for the maser drift and the fit residuals are dominated by white frequency noise. As no high stability local oscillator other than HM2 was running at IT during fountain evaluation period, it is difficult to prove the two positions reported above. However, with the help of all the data collected during the past fountain evaluations and the operative life of HM2, one can reasonably asses that, for a 10-days long period, the fit residuals are dominated by the white frequency noise of the fountain and higher order drifts of the maser are negligible. Final results of the statistical analysis is reported in Table 2:

	Value	**Uncertainty**
Coefficient A	$+2.05 \cdot 10^{-15}$ /day	$0.19 \cdot 10^{-15}$ /day
Coefficient B	$+471.9 \cdot 10^{-15}$	$0.8 \cdot 10^{-15}$

Table 2. Results of the weighted linear fit y=At+B. Data corrected only for density shift.

Local link and dead time uncertainty (ul/lab)

The HM2 is phase compared to UTC(IT) time scale, which is the reference time scale for remote time and frequency transfer tools, with a Time Interval Counter in the INRiM Time and Frequency laboratory. This comparison introduces a uncertainty contribution to the IT-CsF1 transfer to TAI, which is estimated as $0.15 \cdot 10^{-15}$ for this evaluation period (15 days).

Dead time in fountain operation introduces a further uncertainty to the frequency transfer to TAI. The estimation of this uncertainty contribution requires the knowledge of the HM2 noise properties. A conservative estimation is possible using, for example, the stability analysis of the *y(IT-CsF1)-y(HM2)* data obtained during the fountain comparison experiment in 2004 [10]. This analysis provides that the stability of HM2 could be modelled in terms of Allan variance, as:

$$\sigma_y^2(\tau) = \sigma_{yWF}^2(\tau) + \sigma_{yFF}^2(\tau) + \sigma_{yRW}^2(\tau)$$

where $\sigma^2_{yWF}(\tau)$, $\sigma^2_{yFF}(\tau)$ and $\sigma^2_{yRWF}(\tau)$ are respectively the contribution due to white, flicker and random walk frequency noise.A conservative estimation of these contributions is:

$$\begin{aligned} \sigma_{yWF}(\tau) &= 3 \cdot 10^{-13} \tau^{-1/2} \\ \sigma_{yFF}(\tau) &< 3 \cdot 10^{-16} \\ \sigma_{yRW}(\tau) &< 2 \cdot 10^{-19} \tau^{1/2} \end{aligned} \qquad (3)$$

The dead time uncertainty contribution is calculated with a new and improved technique. Starting from the theory reported in [11], an automated software routine [12], implementing a refined algorithm with respect to [11], can handle the actual dead time distribution of the fountain run and provide an estimation of dead time uncertainty.
The dead time uncertainty contribution, calculated for the distribution shown in Fig 2 using the software routine [12] is reported in the table below

Contribution	**Uncertainty (10^{-15})**
HM link to UTC(IT)	0.15
Fountain Dead Time(18%)	0.2
Total (ul/lab)	**0.2**

Table 3. Contributions to ul/lab.

Summary of TAI evaluation results

The final evaluation is obtained using the data reported in Table 2 ($+471.9 \cdot 10^{-15}$), minus for the final correction value reported in Table 1 ($+43.4 \cdot 10^{-15}$).

MJD Period	y(ITCsF1-HM2)	uA	uB	ul/lab
54774-54789	$+428.5 \cdot 10^{-15}$ (*)	$0.8 \cdot 10^{-15}$ (**)	$0.7 \cdot 10^{-15}$	$0.2 \cdot 10^{-15}$ (***)

Table 4. Final results of IT-CsF1 evaluation.

(*) HM2 has the BIPM code 1401102
(**) Including collisional shift evaluation uncertainty (Type A contribution)
(***) Including contribution of uncertainties due to the local link to UTC(IT) and to the fountain dead time.

References

[1] F. Levi, L. Lorini, D. Calonico, A. Godone, "IEN-CsF1 accuracy evaluation and Two-Way frequency comparison". IEEE Transactions on Ultrasonics, Ferroelectrics, and Frequency Control, vol. 51, no. 10, pp. 1216-1224 (October 2004)

[2] F. Levi, L. Lorini, D. Calonico, A. Godone "IEN-CsF1 primary frequency standard at INRIM: accuracy evaluation and TAI calibrations" Metrologia 43 No 6 (December 2006) 545-555

[3] F. Levi, D. Calonico, L. Lorini, S. Micalizio, A. Godone: "Measurement of the blackbody radiation shift of the ^{133}Cs hyperfine transition in an atomic fountain". Phys. Rev. A, Vol. 70, p. 033412, 2004.

[4] E. Simon, P. Laurent and A. Clairon, "Measurement of the Stark shift of the Cs hyperfine splitting in an atomic fountain" Phys. Rev. A 57, 436 (1998).

[5] S. Micalizio, A. Godone, D. Calonico, F. Levi, L. Lorini: "Blackbody radiation shift of the ^{133}Cs hyperfine transition frequency". Phys. Rev. A, Vol. 69, p. 053401, 2004.

[6] D. Calonico, A. Cina, I. H. Bendea, F. Levi, L. Lorini, and A. Godone "Gravitational red-shift at INRIM, Italy". Metrologia 44, L44-L48, 2007.

[7] J. Vanier and C. Audoin, "The Quantum Physics of Atomic Frequency Standards". Bristol/Philadelphia: Adam Hilger, 1989.

[8] S. R. Jefferts, T. P. Heavner, E. A. Donley and T. E. Parker. "Measurement of Dynamic End-to-End Cavity Phase Shifts in Cesium-Fountain Frequency Standards" IEEE transactions on ultrasonics, ferroelectrics, and frequency control, vol. 51, no. 6, June 2004

[9] S.R. Jefferts, J.H. Shirley, N. Ashby, E.A. Burt, and G.J. Dick, "Power dependence of distributed cavity phase induced frequency biases in atomic fountain frequency standards" IEEE T. UFFC 52 2314-2321 (2005)
J.H. Shirley, F. Levi, T.P. Heavner, D. Calonico, D.Yu, and S.R. Jefferts, "Microwave Leakage Induced Frequency Shifts in the Primary Frequency Standards NIST-F1 and IEN-CSF1". IEEE T. UFFC 53 2376-2385 (2006)

[10] A. Bauch, J. Achkar, S. Bize, D. Calonico, R. Dach, R. Hlavac, L. Lorini, T. Parker, G. Petit, D. Piester, K. Szymaniec and P. Uhrich, "Comparison between frequency standards in Europe and the USA at the 10^{-15} uncertainty level". Metrologia 43 No 1 (February 2006) 109-120

[11] Dai-Hyuk Yu, Marc Weiss and Thomas E Parker, "Uncertainty of a frequency comparison with distributed dead time and measurement interval offset" Metrologia 44 No 1 (February 2007) 91-96

[12] G. Panfilo, T. Parker, Proc. 2007 Joint Mtg. IEEE Intl. Freq. Cont. Symp. and EFTF Conf., 805-810, 2007
T. Parker, G. Panfilo, Proc. 2007 Joint Mtg. IEEE Intl. Freq. Cont. Symp. and EFTF Conf., 986-991, 2007